2

AD-A221 545

DOCUMENTATION PAGE

Form Approved
OMB No. 0704-0188

1a. REPORT SECURITY CLASSIFICATION
Unclassified

1b. RESTRICTIVE MARKINGS
None

2a. SECURITY CLASSIFICATION AUTHORITY

2b. DECLASSIFICATION / DOWNGRADING SCHEDULE

3. DISTRIBUTION / AVAILABILITY OF REPORT
Approved for public release; distribution unlimited

4. PERFORMING ORGANIZATION REPORT NUMBER(S)

5. MONITORING ORGANIZATION REPORT NUMBER(S)
AFOSR-TR- 90-0480

6a. NAME OF PERFORMING ORGANIZATION
Electrical Engineering Dept.
Columbia University

6b. OFFICE SYMBOL *(If applicable)*
N/A

7a. NAME OF MONITORING ORGANIZATION
Air Force Office of Scientific Research

6c. ADDRESS *(City, State, and ZIP Code)*
1320 Mudd Building
Columbia University
New York, N.Y. 10027

7b. ADDRESS *(City, State, and ZIP Code)*
Bld 410
Bolling Air Force Base, D.C. 20332-6448

8a. NAME OF FUNDING / SPONSORING ORGANIZATION
Air Force Office of Scientific Research

8b. OFFICE SYMBOL *(If applicable)*

9. PROCUREMENT INSTRUMENT IDENTIFICATION NUMBER
AFOSR-89-0215

8c. ADDRESS *(City, State, and ZIP Code)*
Bld 410
Bolling Air Force Base, D.C. 20332-6448

10. SOURCE OF FUNDING NUMBERS

PROGRAM ELEMENT NO	PROJECT NO.	TASK NO	WORK UNIT ACCESSION NO
61102F	2917	A3	

11. TITLE *(Include Security Classification)*
"Molecular Beam Epitaxial Growth, Characterization, and Devices of Modulated Semiconductor Structures"

12. PERSONAL AUTHOR(S)
Wen I. Wang

13a. TYPE OF REPORT
Final

13b. TIME COVERED
FROM 02/1/89 TO 1/31/90

14. DATE OF REPORT *(Year, Month, Day)*
2/28/90

15. PAGE COUNT

16. SUPPLEMENTARY NOTATION
AFOSR-89-0215

17. COSATI CODES

FIELD	GROUP	SUB-GROUP

18. SUBJECT TERMS *(Continue on reverse if necessary and identify by block number)*

19. ABSTRACT *(Continue on reverse if necessary and identify by block number)*

Key Words: Molecular Beam Epitaxy, X-ray diffraction, RHEED, GeSn, AlGaSb, Surface Structure

1990
D

20. DISTRIBUTION / AVAILABILITY OF ABSTRACT
☒ UNCLASSIFIED/UNLIMITED ☐ SAME AS RPT. ☐ DTIC USERS

21. ABSTRACT SECURITY CLASSIFICATION
Unclassified

22a. NAME OF RESPONSIBLE INDIVIDUAL
~~Prof. Wen I. Wang~~ Pomrenke

22b. TELEPHONE *(Include Area Code)*
202-854-1748

22c. OFFICE SYMBOL
NE

DD Form 1473, JUN 86

Previous editions are obsolete.

SECURITY CLASSIFICATION OF THIS PAGE

Air Force Office of Scientific Research

Technical Report

Equipment Grant No. AFOSR-89-0215

"Molecular Beam Epitaxial Growth, Characterization, and Devices of Modulated Semiconductor Structures"

by

Wen I. Wang, Principal Investigator

Professor

Department of Electrical Engineering

Columbia University

New York, NY 10027

Final report for equipment grant no. AFOSR-89-0215 "Molecular beam epitaxial growth, characterization, and devices of modulated semiconductor structures"

A double-crystal x-ray diffractometer was installed at Columbia as a key element of the materials characterization effort supporting the molecular beam epitaxy research program. This equipment so far has been used in the study of metastable GeSn alloys grown on InP and GaSb substrates, and in analysis of the (Al, Ga)Sb material system.

1. Molecular Beam Epitaxial Growth of Metastable $Ge_{1-x}Sn_x$ Alloys. The growth of $Ge_{1-x}Sn_x$ alloys is of increasing interest because of the potential for applications of this material to infrared detectors. With its narrow band gap (0 - 0.5 eV) and high mobility, $Ge_{1-x}Sn_x$ is an attractive alternative to the ternary $Hg_x Cd_{1-x} Te$. Substrate stabilized metastable single crystal $Ge_{1-x}Sn_x$ films can be grown by molecular beam epitaxy (MBE). We have grown for the first time single crystal $Ge_{1-x}Sn_x$ alloys on lattice matched GaSb (with $x=0.5$) and InP (with $x=0.26$) substrates up to a thickness of 0.3 µm. Reflection high energy electron diffraction (RHEED) observations and x-ray measurements show that even at very small lattice mismatch (less than 0.05%), single crystal $Ge_{1-x}Sn_x$ films cannot be grown thicker than 0.3 µm. Our x-ray results suggest that the critical thickness of α-Sn and $Ge_{1-x}Sn_x$ single crystal films is mainly determined

by a phase transition mechanism, and the dislocation generation equivalent critical thickness is an overestimate. Under practical MBE growth conditions, it is very difficult to grow thick films, due to the sensitivity of the critical thickness to composition fluctuations. We have shown that even under an exact lattice match between substrate and film, the critical film thickness is limited.

There are three factors that make the growth of metastable single crystal $Ge_{1-x}Sn_x$ alloys difficult. First, the maximum equilibrium solubilities of Sn in Ge and Ge in Sn are about 1 at% and 0.6 at%, respectively. Second, Sn is an allotropic element that transforms from semiconducting α-Sn (diamond structure) to metallic β-Sn (body-centered tetragonal structure) at 13.2 °C. A relatively low growth temperature is required because the system is a simple eutectic, in which the invariant point occurs at a composition close to that of pure Sn and at a temperature about 1 °C below the melting point of β-Sn, 232 °C. Third, as the tin composition is increased, the relatively high diffusivity of Sn in Ge and the free energy difference between the metastable state and the equilibrium two-phase state cause phase separation and an α to β transformation.

Throughout these studies, RHEED was used to monitor the growth in-situ, while x-ray diffraction was used to characterize the as-grown alloy quality. Double-crystal x-ray rocking curve measurements of the films show a distinct alloy peak, which disappears after heat treatment, indicating phase segregation into the more stable two-phase state. An additional weaker feature in the x-ray data may represent a segragated phase corresponding to a region of different alloy composition.

2. Surface Structures of the (Al, Ga)Sb Material System. We have studied the surface structures of GaSb, AlGaSb, and alternating GaSb/AlSb layers using 10 kV reflection electron diffraction. Above 540^{O}C, the Sb-stabilized surface (1x3) patterns change to *c*(8x2), a Ga-stabilized surface. Because the *c* (8x2) surface has been observed on all other III-V arsenides, phoshpides, and antimonides, it is now clear that the *c*(8 x 2) metal-stabilized surface is common to all III-V compounds, suggesting that bond-pairing occurs on all III-V semiconductor surfaces and is a universal reconstruction mechanism. The smooth, sharp transitions observed in the growth of alternating GaSb and AlSb layers show that atomically smooth interfaces can be formed in this system. In contrast, for the AlAs overgrowth on GaAs transient structures associated with a Ga surface layer can be observed.

The "two-by" reconstructions are interpreted as evidence of the lone-pair dangling bonds of the surface group V atoms. Of course, the same bond-pairing phenomenon should occur for AlAs, which has the same zincblende structure and is lattice-matched to GaAs. By raising the growth temperature to above 800 ^{O}C, a reproducible *c*(8x2) pattern is obtained for the metal-stabilized surface, exactly as for GaAs. Thus, despite the completely different surface structures at lower temperatures for GaAs and AlAs, the same *c*(8x2) reconstruction could be observed at high temperatures. The disordered surface of AlAs at low substrate temperature is clearly due to the excess As that bonds to Al, the reduced migration length of Al adatoms, and therefore the reduced ability to find the right lattice sites, all of which are due to the stronger bond energy of AlAs compared to GaAs. Since the observation of the *c*(8x2) AlAs surface, it was considered possible that the *c*(8x2) reconstruction is a universal feature of III-V semiconductor surfaces.

We studied AlSb and GaSb grown from elemental Ga and Al, and Sb_4 sources. We observed that the *c* (2x6) structure is the dominant surface phase for substrate temperatures between 400 ^{o}C and 600 ^{o}C under Sb-stabilized conditions. Above 540 ^{o}C, depositing sub-monolayer quantities of Ga on the Sb-stabilized surface changed the *c* (2x6) pattern to (1x3). With further Ga deposition the pattern changed to *c* (8x2), a Ga-stabilized surface (Figure 1). Even with the higher growth temperature, the *c* (8x2) pattern is not completely reproducible. Thus, a temperature of 540 ^{o}C is a necessary but not sufficient condition for obtaining this pattern. Nonetheless, our results show for the first time that the *c* (8x2) metal-stabilized surface, which has been observed on all other III-V arsenides, phosphides, and antimonides, is in fact a universal feature of III-V compound surfaces. This evidence suggests that bond-pairing occurs on all (100) III-V surfaces and may even be a universal reconstruction for surfaces of all tetrahedrally coordinated semiconductors.

Presentations and publications:

1. J. Piao, R. Beresford, and W.I. Wang, "Surface structures of the (Al,Ga)Sb systems", 10th Molecular Beam Epitaxial Workshop, Sept. 13-15, 1989, North Carolina State University, Raleigh, N.C. Also, to be published in J. Vac. Sci. Tech. B March/April issue, 1990.

2. J. Piao, R. Beresford, W.I. Wang, H. Homma, "Molecular beam epitaxial

growth of metastable GeSn alloys", Sept. 13-15, 1989, North Carolina State University, Raleigh, N.C. Also to be published in J. Vac. Sci. Tech. March/April issue, 1990.

J. Vac Science & Tech

Molecular Beam Epitaxial Growth of Metastable $Ge_{1-x}Sn_x$ Alloys

J. Piao, R. Beresford, T. Licata, and W. I. Wang
Department of Electrical Engineering and Microelectronics Sciences
Laboratories, Columbia University, New York, NY, 10027

H.Homma
Department of Physics, Brooklyn College - CUNY, New York, NY 11210

Abstract

Substrate stabilized metastable single crystal $Ge_{1-x}Sn_x$ films can be grown by molecular beam epitaxy (MBE). We have grown for the first time single crystal $Ge_{1-x}Sn_x$ alloys on lattice matched GaSb (with x=0.5) and InP (with x=0.26) substrates up to a thickness of 0.3 µm. Reflection high energy electron diffraction (RHEED) observations and x-ray measurements show that even at very small lattice mismatch (less than 0.05%), single crystal $Ge_{1-x}Sn_x$ films cannot be grown thicker than 0.3 µm. Our x-ray results suggest that the critical thickness of α-Sn and $Ge_{1-x}Sn_x$ single crystal films is mainly determined by a phase transition mechanism, and the dislocation generation equivalent critical thickness is an overestimate. Under practical MBE growth conditions, it is very difficult to grow thick films, due to the sensitivity of the critical thickness to composition fluctuations. We have shown that even under an exact lattice match between substrate and film, the critical film thickness is limited.

[illegible]: [illegible] Single Crystals [illegible], Antimony, X-ray [illegible], Aluminum [illegible] Tin), Surface Structure [illegible] (JC)

I. Introduction

The growth of $Ge_{1-x}Sn_x$ alloys is of increasing interest because of the potential for applications of this material to infrared detectors. With its narrow band gap (0 - 0.5 eV) [1] and high mobility, $Ge_{1-x}Sn_x$ is an attractive alternative to the ternary $Hg_x Cd_{1-x} Te$. The $Ge_{1-x}Sn_x$ system is also important for investigating the growth of non-isostructural substitutional crystalline metastable alloys [2].

Although many researchers have used various growth methods [2-7], the highest Sn composition reported to date in a single-crystal $Ge_{1-x}Sn_x$ alloy is 8% [2,5]. The MBE growth of metastable alloys was first studied by Farrow et al.[3] and later by Pukite et al.[4] and Asom et al.[5]. All of the films grown were limited to a thickness of less than 1 μm. We grew alloy layers of various thicknesses and compositions, and found that a single-crystal $Ge_{1-x}Sn_x$ alloy, with Sn composition up to 0.56 and thickness less than 3000 Å can be grown under certain conditions. In this discussion, we present the problems in alloy growth as seen in our RHEED, x-ray, and surface morphology observations.

There are three factors that make the growth of metastable single crystal $Ge_{1-x}Sn_x$ alloys difficult. First, the maximum equilibrium solubilities of Sn in Ge and Ge in Sn are about 1 at% [8] and 0.6 at% [9], respectively. Second, Sn is an allotropic element that transforms from semiconducting α-Sn (diamond structure) to metallic β-Sn (body-centered tetragonal structure) at 13.2 ^{0}C [10]. A relatively low growth temperature is required because the system is a simple eutectic, in which the invariant point occurs at a composition close to that of pure Sn and at a temperature about 1 ^{0}C below the melting point of β-Sn, 232 ^{0}C. Third, as the tin composition is increased, the relatively high diffusivity of Sn in Ge and the free energy difference between the metastable state and the equilibrium two-phase state cause phase separation and an α to β transformation.

II. Growth and Characterization

$Ge_{1-x}Sn_x$ alloys of various Sn compositions were grown on various substrates at different substrate temperatures in our Varian GEN II MBE system. Throughout these studies, RHEED was used to monitor the growth in-situ, while x-ray diffraction and surface morphology were used to characterize the as-grown alloy quality. The substrates used were (001)-oriented InP and GaSb. The InP substrates are 3° off the (100) axis. The substrate temperature was kept between 150 and 350 ^{0}C, depending on the desired Sn composition and the substrate used. During the alloy growth, the background pressure was kept to less than 2×10^{-9} Torr.

The InP substrates were cleaned at temperatures of 500-520 °C. Following substrate surface cleaning the Sn and Ge effusion cell temperatures were adjusted to give an arrival rate of Sn and Ge atoms equivalent to an overall growth rate of 0.3-1 μm/h. Figure 1 shows RHEED patterns recorded along ‹110› azimuth for the InP surface after surface cleaning [Fig.1a] and the $Ge_{1-x}Sn_x$ film after 0.3 μm overgrowth [Fig.1b]. The (2x4) RHEED pattern of the InP changed to (1 x 1) symmetry immediately after growth commenced and remained for a thickness of 0.3 μm. No change in the spacing of the diffraction streaks was observed during the growth up to 0.3 μm, indicating that the film is single crystal. The growth temperature used in this case was 200 °C. The composition estimated from x-ray data agrees well with electron microprobe data, giving a value of x=0.26. As the film thickness was increased further, the diffraction streaks became diffuse and showed some evidence of a departure from cubic symmetry, indicating the presence of the β-Sn phase. The observation of a strongly streaked (1 x 1) RHEED pattern during the film growth suggests that the growth occurs by a two-dimensional layer mechanism, confirming the earlier observations by Farrow et al. [3].

Figure 2 shows RHEED patterns of the tilted GaSb substrate after surface cleaning [Fig.2a] and $Ge_{1-x}Sn_x$ film after 500 Å overgrowth [Fig.2b]. The substrate temperature was 190 °C. The composition obtained from the electron microprobe data is x=0.54.

Figure 3(a) shows the double crystal x-ray rocking curve of a $Ge_{0.74}Sn_{0.26}$ film about 0.36 μm thick deposited on InP. Figure 3(b) shows the same film after heat treatment at 450 °C. The alloy peak disappeared after the treatment, indicating phase segregation into the more stable two-phase state. We find that in further growth beyond 0.3 μm the β-Sn phase segregates, leading to spotty and diffuse RHEED patterns. The small peak marked Y' in Fig. 3(a) may represent a segragated phase corresponding to a region of different alloy composition [5]. Figures 4(a) and 4(b) show Nomarski microphotographs of the surface morphology before and after the heat treatment.

Figure 5 shows Nomarski microphotographs of the surface morphology of three alloy films with different thicknesses. Small droplets are evident on the samples with the β-Sn phase. The thicker the layer, the larger and denser are these droplets.

III. Lattice Mismatch and Critical Thickness

Pseudomorphic growth of the $Ge_{1-x}Sn_x$ alloy is limited by two factors. One is the generation of misfit dislocations at the interface. The other more important factor for this system is phase separation and the structural phase transformation from α-Sn to β-Sn.

In the MBE growth of heterostructures, it is well known that if the lattice mismatch between the substrate and the epitaxial layer is small, the first monolayer is forced to be commensurate with the substrate.

Successive overlayers will lattice match to the chemically identical layer immediately below and hence also be in a state of uniform strain. However, as the layer thickness increases to a critical value h_c, the coherent homogeneous strain energy becomes so large that it is energetically more favorable to accommodate a fraction of the misfit by a periodic array of defects than to strain additional layers into coherence with the substrate. A much reduced strain then remains in the overlayer.

In this case, the defect is called a misfit dislocation. In the simplest atomic picture, one edge misfit dislocation corresponds to either one extra row (if the lattice constant of the overlayer is the smaller one) or one missing row of atoms in the interfacial plane perpendicular to the direction of misfit. The misfit dislocation density continues to increase until the average strain in the overlayer is reduced to zero, that is, the lattice constant of the epitaxial layer is equal to its bulk crystal value.

The existence of a critical thickness in heteroepitaxy was first studied by Van de Merwe [11] and later by numerous authors for the Ge_xSi_{1-x} and $In_{1-x}Ga_xAs$ systems. Calculations by Van de Merwe and Ball [12,13] and by Matthews [14-16] were based on thermodynamic equilibrium between a grid of interfacial misfit dislocations and the strained epitaxial film. Work on the $In_{1-x}Ga_xAs$ system [17] suggested that the critical thickness of this system obeys the Matthews mechanical equilibrium theory [14,15], while Ge_xSi_{1-x} obeys reasonably well the energy balance theory, which was first proposed by Van de Merwe, then modified by numerous authors [18-20].

The Matthews mechanical equilibrium theory is based on the assumption that grown-in threading dislocations from the substrate are the origin of the misfit dislocations. For the half-loop nucleation, the force exerted by misfit stress is balanced by the tension in the dislocation line. This theory underestimates the critical thickness for Ge_xSi_{1-x}, but gives a reasonable value for $In_{1-x}Ga_xAs$.

In the energy balance theory, the total free energy of the epilayer system is zero at the critical thickness. Van de Merwe first obtained an expression for h_c based on the assumption that the interfacial energy is the minimum energy available for the generation of dislocations. Dislocations at the film/substrate interface will begin to be generated when the interfacial energy equals the areal strain energy density.

Recently, several energy balance theories have been proposed [18-20]. All these theories assume that semicircular dislocations nucleate at the epilayer surface, expand to the interface by glide processes, and finally create misfit dislocations. Although Van de Lear et al. [20] discussed the kinetic effect (the nucleation barrier, or free energy maximum) all of these derivations of the critical thicknesses are based on thermodynamic equilibrium considerations. People et al. [19] gave an empirical expression for the critical thickness of Ge_xSi_{1-x} based on the assumption that a misfit dislocation will be generated in the overlayer if the strain energy is equal to an isolated screw dislocation energy. Although these energy balance theories fit well with the experimental results of Bean et al. [21], the types of dislocation (screw, edge, or 60° mixed) that are actually present are not clear yet.

The critical thicknesses for Sn and $Ge_{1-x}Sn_x$ differ from those of Ge_xSi_{1-x} and $In_{1-x}Ga_xAs$ because of the structural phase transition of Sn. In the latter systems, with exact lattice matching one can expect to grow very thick single-crystal dislocation free overlayers. Such is not the case for Sn and $Ge_{1-x}Sn_x$. Even with an exact lattice match, h_c is limited. The dislocation-controlled critical thickness is an upper bound on the true critical thickness.

A. Pure Sn System[22].

Pseudomorphic stabilization of a metastable phase is possible when the system will have a lower free energy if the thin film has a metastable crystal structure, suitably related to the crystal structure and parameters of the substrate, than if it had its stable crystal structure. α-Sn is metastable with respect to the metallic β-Sn above 13.2 °C. α-Sn has the diamond structure with a lattice constant of 6.489 Å at 25 °C; β-Sn has the body centered tetragonal crystal structure with a=5.8311 Å and c=3.1817 Å. For the substrate CdTe (a=6.48 Å), an appreciable elastic distortion is required for the β-Sn lattice to match coherently. This elastic distortion has an associated energy that adds to the free energy of the β-Sn/substrate film system an amount proportional to the thickness of the film. When this total distortional energy per unit area of the film exceeds the interface energy associated with the non-coherency between the β-Sn film and the substrate, then there will be a driving force for the film/substrate interface to generate misfit dislocations and non-coherency.

On the other hand, the α-Sn/substrate film system has no strain energy and the interface energy is nil or negative. The only positive contribution to the free energy relative to the α-Sn/CdTe system is the lattice stability energy (the difference in free energy between the α and β polymorphs of Sn), which is also proportional to the thickness of the film. These considerations lead to the posibility of stabilizing the metastable structure as described schematically in Fig. 5. In this figure we have assumed that the coherent interfaces in both cases have negligible energy. Thus, if the lattice stability energy density is smaller than the strain energy density that would be induced in the coherent stable phase, then there exists a range of film thickness over which the metastable phase can be pseudomorphically stabilized. Conversely, if the strain energy density is smaller then the metastable phase cannot be stabilized at any thickness.

At the critical thickness,

$$h^* g_\beta + \Delta\sigma = h^* g_\alpha$$

$$h^* = \frac{\Delta\sigma}{g_\alpha - g_\beta}$$

where

$$\Delta\sigma = \sigma_i^\beta - \sigma_i^\alpha + \sigma_s^\beta - \sigma_s^\alpha$$

and $\sigma^\beta{}_i$, $\sigma^\alpha{}_i$ are the interfacial energy of β-Sn and α-Sn, respectively, and $\sigma^\beta{}_S$, $\sigma^\alpha{}_S$ are the strain energy of β-Sn and α-Sn film, respectively. The estimation of critical thickness will be given elsewhere [24].

B. $Ge_{1-x}Sn_x$ System

This is a binary three-phase system, and the critical thickness is much more complicated. A simplified treatment is given here; a more detailed discussion will be given elsewhere. As with pure Sn, the dislocation equivalent critical thickness is an upper limit for $Ge_{1-x}Sn_x$ because the same structural transformation applies, and this transformation is assumed to be the controlling factor for the critical thickness. In the following we apply both energy balance theory and the Matthews mechanical equilibrium theory to estimate an upper limit to the single crystal alloy thickness.

$Ge_{1-x}Sn_x$ has the zincblende structure, like Ge_xSi_{1-x} and $In_{1-x}Ga_xAs$, and we expect that the glide plane is {111}, and the Burgers vector is of the type

$$b = \frac{a}{2}\langle 110\rangle$$

We assume that coherency will break down and dislocations will start to be generated when the areal strain energy density is equal to the energy associated with the formation of an isolated screw dislocation at a distance from the free surface equal to the film thickness *h* [19].

The areal strain energy density associated with a film of thickness *h* is given by

$$\varepsilon_{strain} = 2G\left(\frac{1+\nu}{1-\nu}\right)hf^2$$

where G is the shear modulus, ν is the Poisson ratio, and f is the misfit. The areal energy density associated with an isolated screw dislocation at a distance *h* from a free surface is approximately [23]

$$\varepsilon_{screw} \approx \left[\frac{Gb^2}{8\pi\sqrt{2}\,a(x)}\right]\ln\left(\frac{h}{b}\right)$$

where a(x) is the composition dependent lattice constant of $Ge_{1-x}Sn_x$ alloys. Equating the above expressions, with $h=h_c$, $\langle a(x)\rangle=6.0731$ Å, and $b=4.29$ Å, we obtain

$$h_c = \left[\frac{1.73\times10^{-2}\ \text{Å}}{f^2}\right]\ln\left(\frac{h_c}{4.29}\right)$$

This equation is ploted in Fig. 7 for the alloy on InP.

We apply Matthews theory for the half-loop dislocation generation to obtain the following equation:

$$h_c = \frac{11}{16\pi}\frac{4.29}{f}\left[\ln\left(\frac{h_c}{4.29}\right)+1\right]$$

This equation is ploted in Fig.8 for the alloy on InP.

IV. Discussion

In the previous section we assumed that in $Ge_{1-x}Sn_x$, the critical thickness is mainly determined by the structural phase transition, obtaining thereby an upper limit of critical thickness. Consideration of the kinetics (mainly the nucleation barrier) will give a slightly larger value of h_c.

The equilibrium phases in the pure Sn and $Ge_{1-x}Sn_x$ systems are the single β-Sn phase and the two phase mixture, respectively [24]. The pseudomorphic stabilization of metastable phases in the thin epilayers is due to the effect of the film/substrate interfacial energy and the strain energy. The substrate influence is very significant, as can be seen for the following two examples. Prinz [25] showed that a GaAs (110) surface can support epitaxial growth of bcc cobalt up to a thickness approaching 0.1 µm before the film transforms to its bulk hcp phase. The other example is the epitaxial growth of superconducting Nb_3Nb on silicon [26]—an A15 compound that does not exist in the bulk.

In $Ge_{1-x}Sn_x$, the heat of formation is positive [24], and the equilibrium state of the bulk material is always a phase mixture. When considering the film/substrate system, the strain energy introduced by the difference in lattice parameters of the two phases plays the critical role in stabilizing the single phase α-Sn and $Ge_{1-x}Sn_x$. This strain energy will reverse the sign of

$$\frac{\partial^2 G}{\partial x^2}$$

and hence prevent spinodal decomposition in the $Ge_{1-x}Sn_x$ system.

The volume change of 27% and the change from semiconductor to metallic bonds accompanying the α-β transition suggest that the transition is reconstructive[22]. From Figures 6 and 7, we see that the x vs h_c curve is very steep. A very small composition fluctuation will cause a large reduction in h_c. Consequently, under practical MBE growth conditions (composition fluctuation over the whole film surface of about ±1%), the critical thickness will be about 0.3 µm.

Our x-ray results agree well with this analysis. The peak separation between the $Ge_{1-x}Sn_x$ and InP substrate is only 0.02°. The misfit is thus $f < 0.05\%$. According to the equilibrium theory of "critical thickness" for such a small misfit, one would expect a single crystal film much thicker than 0.3 µm under ideal epitaxial conditions.

V. Summary

We have grown single crystal $Ge_{1-x}Sn_x$ alloys for various substrates and different substrate temperatures with various values of x. Under certain conditions, one can grow single crystal films with x up to 0.5 and thicknesses up to 0.3 µm. Due to the non-equilibrium nature of the MBE growth process, substrate stabilized metastable single crystal $Ge_{1-x}Sn_x$ films can be grown. However, even under exactly lattice matched conditions, only a limited thickness can be obtained. Our x-ray results suggest that the dislocation generation equivalent critical thickness is an upper limit of the film thickness. Under practical MBE growth conditions, the fluctuations in growth parameters will make it difficult to grow even 1 µm thick single crystal films.

We wish to thank E. Machlin for valuable discussions and suggestions on α-Sn critical thickness.

This work is supported by the Air Force Office of Scientific Research(88-0126B and equipment grant 89-0215A), with additional support from the Naval Research Laboratory(N00014-89-K-2020).

References:

1. S.Oguz, William Paul, T.F.Deutsch, B-Y. Tsaur, and D.V. Murphy. Appl. Phys. Lett. 43,848(1983)
2. S.I. Shah, J.E.Greene, L.L.Abels, Qi Yao and P.M. Raccah,J. Crystal Growth 83 ,3(1987)
3. R.F.C. Farrow, D.S.Robertson,G.M.Williams,A.G.Cullis,G.R.Jones,I.M.Young and P.N.J. Dennis,J.Crystal Growth 54,507(1981)
4. P.R.Pukite,Alex Harwit, and S.S. Iyer, Appl. Phys. Lett. 54,2142(1989).
5. M.T.Asom, E.A.Fitzgerald,A.R.Kortan,B.Spear,and L.C.Kimerling Appl.Phys. Lett. 55,578(1989).
6. R.J.Temkin, G.A.N.Connell and W.Paul, Slid State Commun.11,1591(1972)
7. R.J.Temkin and W.Paul, in "Proc. 5th Intern. conf. on Amorphous and Liquid Semiconductors", Garmich Partenkirchen,1973
8. C.D.Thurmond,F.ATrumbore and M.Kowalchik, J.Chem.Phys. 24,799(1956)
9. C.D.Thurmond, J.Phys. Chem. 57, 827(1953)
10. W.klemm and H.Stohr, Z.Anorg.Chem.241,305(1939)
11. Van de Merwe,J.H., J.Appl. Phys. 34,117(1963)
12. Van de Merwe,J.H., Surf. Sci. 31,198(1972)
13. Van de Merwe,J.H. and Ball,C.A.B., in " Epitaxial growth", edited by J.W.Matthews(Academic,New York,1975), part B, chap.6
14. Matthews,J.W., J. Vac. Sci. Technol. 12,126(1975)
15. Matthews,J.W., in "Epitaxial growth", edited by J.W.Metthews(Academic, New York,1975), partB, chap. 8.
16. Metthews,J.W., in "Dislocations in solids", edited by F.R.N. Nabarro(North-Holland, Amsterdam,1979)
17. Fritz,J., Appl. Phys. Lett. 51,1080(1987)
18. P.M.J.Maree,J.C.Barbour,J.F.Van der Veen,K.L.Kavanagh, C.W.T.Bulle-Lieuwma and M.P.A. Viegers, J.Appl.Phys. 62, 4413(1987)
19. R.People and J.C.Bean, Appl. Phys. Lett. 47,322(1985)

20. R.H.M.Van de Leur,A.J.G.Schellingerhout,F.Tuinstra, and J.E.Mooij,J.Appl.Phys. 64,3043(1988)

21. J.C. Bean, L.C. Feldman, A.T. Fiory, S.Nakahara, and I.K. Robinson, J.Vac. Sci. Technol. A2,436(1984).

22. E. Machlin (Private communication).

23. F.R.N. Nabarro, "Theory of crystal dislocations(clarendon, oxford1967), P.75.

24. J. Piao, E. Machlin, W.I. Wang (unpublished).

25. G.A. Prinz, Phys. Rev. Lell. 54, 1051(1985)

26. G.R. Stewart,L.R. Newkirk and F.A. Valencia, Phys. Rev.B21,5055(1980).

Figure Captions:

Fig. 1. RHEED pattern of the 3° tilted (001)-oriented InP substrate after surface cleaning (a) and after overgrowth of 0.3 µm of $Ge_{0.74}Sn_{0.26}$ film (b).

Fig.2. RHEED pattern of the tilted GaSb substrate after surface cleaning (a) and after overgrowth of 500 Å $Ge_{0.5}Sn_{0.5}$ film (b).

Fig. 3. Double crystal x-ray rocking curve of $Ge_{0.74}Sn_{0.26}$ film of about 0.36 µm thickness deposited on a 3° off (001) InP substrate (a). Rocking curve for same film after heat treatment at 450 °C (b).

Fig.4. Nomarski microphotographs of the surfase mophology of $Ge_{0.74}Sn_{0.26}$ film of 0.36 µm thickness depsited on a 3° off (001)-oriented InP substrate (a). Morphology for same film after heat treatment at 450 °C (b). Magnification is 1500.

Fig.5. Nomarski microphotographs of the surface mophology of the three alloy films with different thickness: 0.36 µm (a), 0.6 µm (b), 1.2 µm (c). Magnification is 1500.

Fig.6. Schematic plot of free energy versus film thickness for α-Sn/substrate and β-Sn/substrate systems, illustrating the critical thickness of the α-Sn film.

Fig.7. $Ge_{1-x}Sn_x$ critical thickness vs Sn composition for film grown on InP substrate (energy balance theory).

Fig.8. $Ge_{1-x}Sn_x$ critical thickness vs Sn composition curve for film grown on InP substrate (mechanical equilibrium theory).

Fig 1

Fig 2

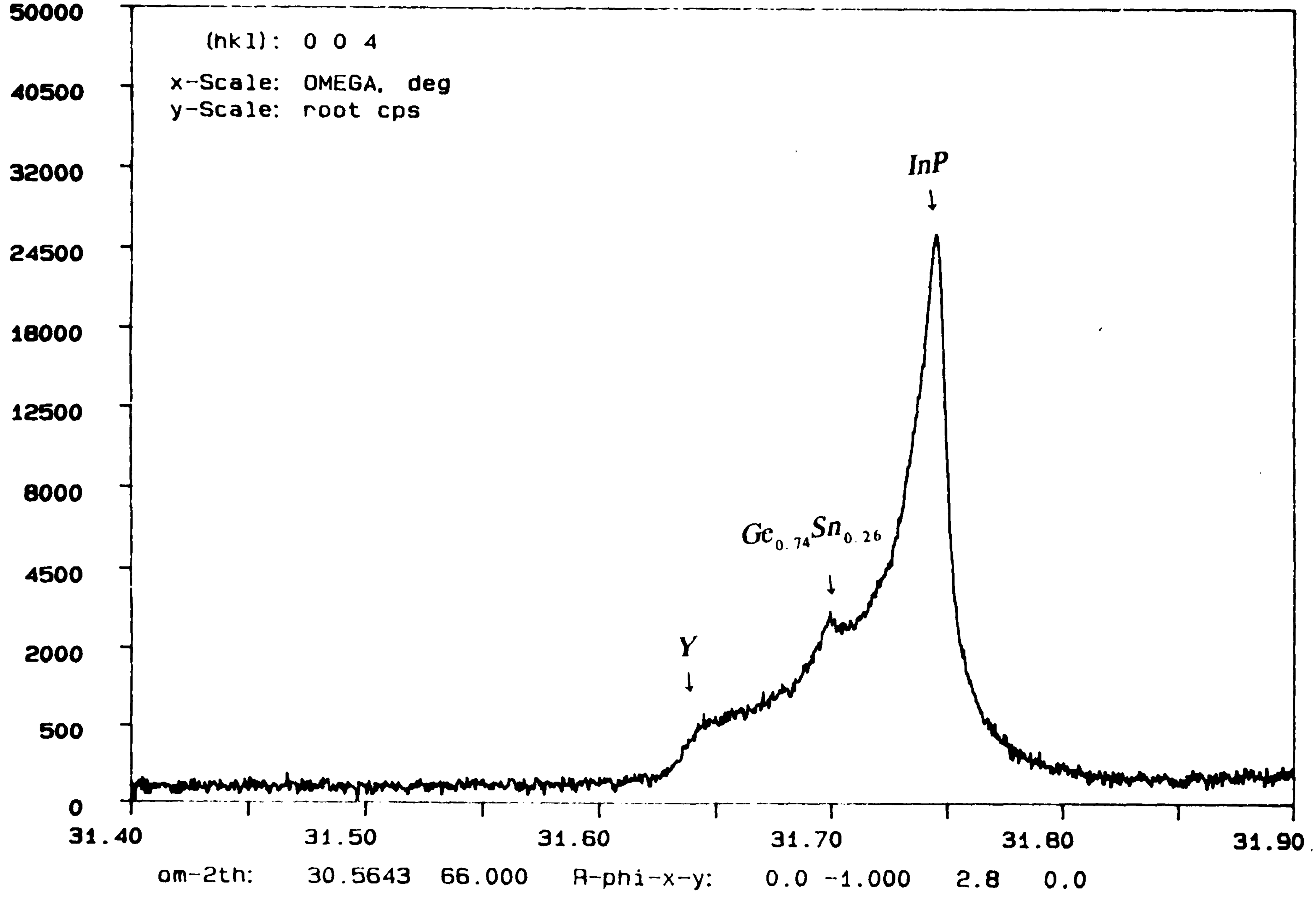
50000
40500
32000
24500
18000
12500
8000
4500
2000
500
0
(hkl): 0 0 4
x-Scale: OMEGA, deg
y-Scale: root cps
InP
$Ge_{0.74}Sn_{0.26}$
Y
31.40
31.50
31.60
31.70
31.80
31.90
om-2th: 30.5643 66.000 A-phi-x-y: 0.0 -1.000 2.8 0.0

Fig. 3a

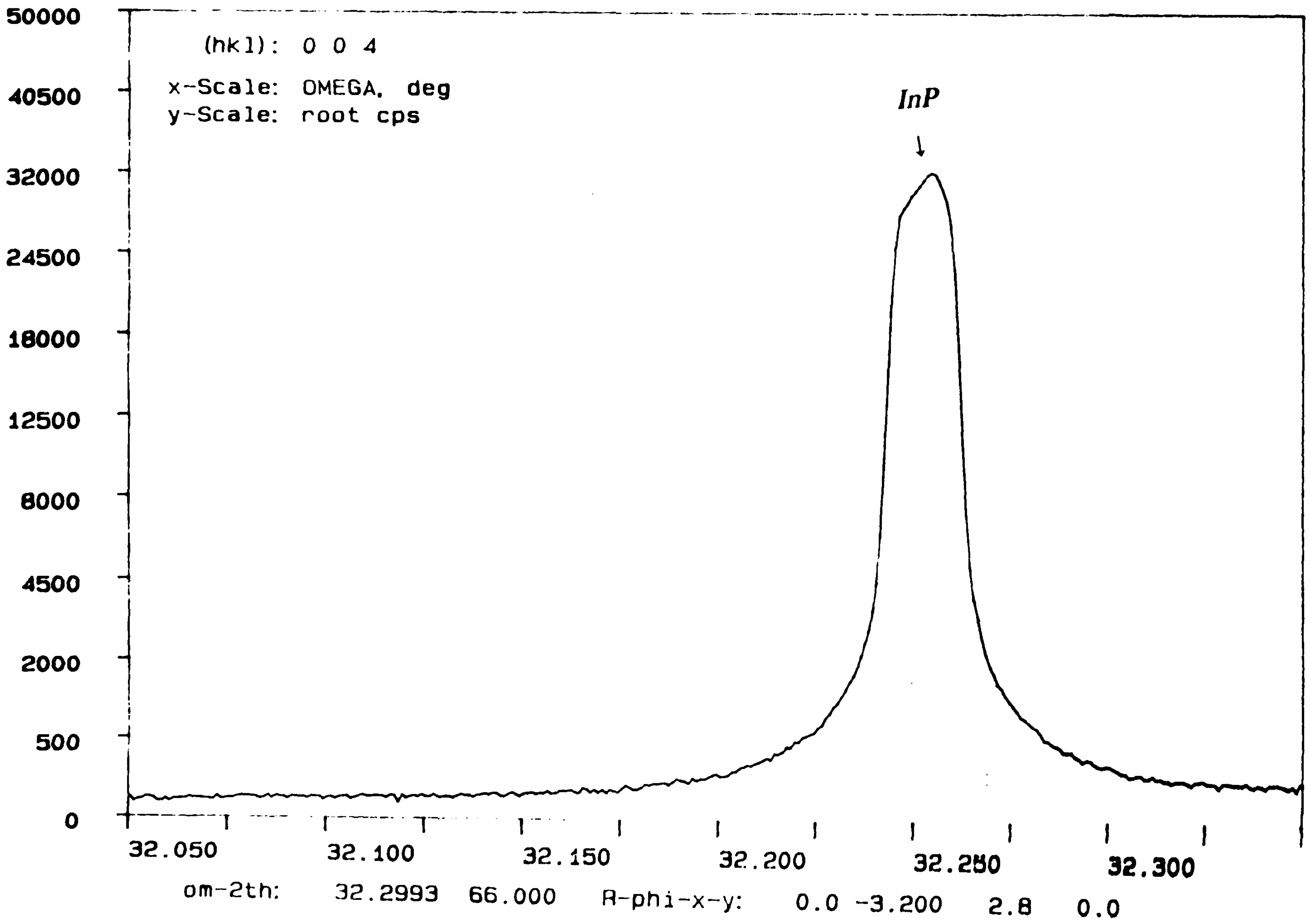
50000
40500
32000
24500
18000
12500
8000
4500
2000
500
0
(hkl): 0 0 4
x-Scale: OMEGA, deg
y-Scale: root cps
InP
32.050
32.100
32.150
32.200
32.250
32.300
om-2th: 32.2993 66.000 R-phi-x-y: 0.0 -3.200 2.8 0.0

Fig 3b.

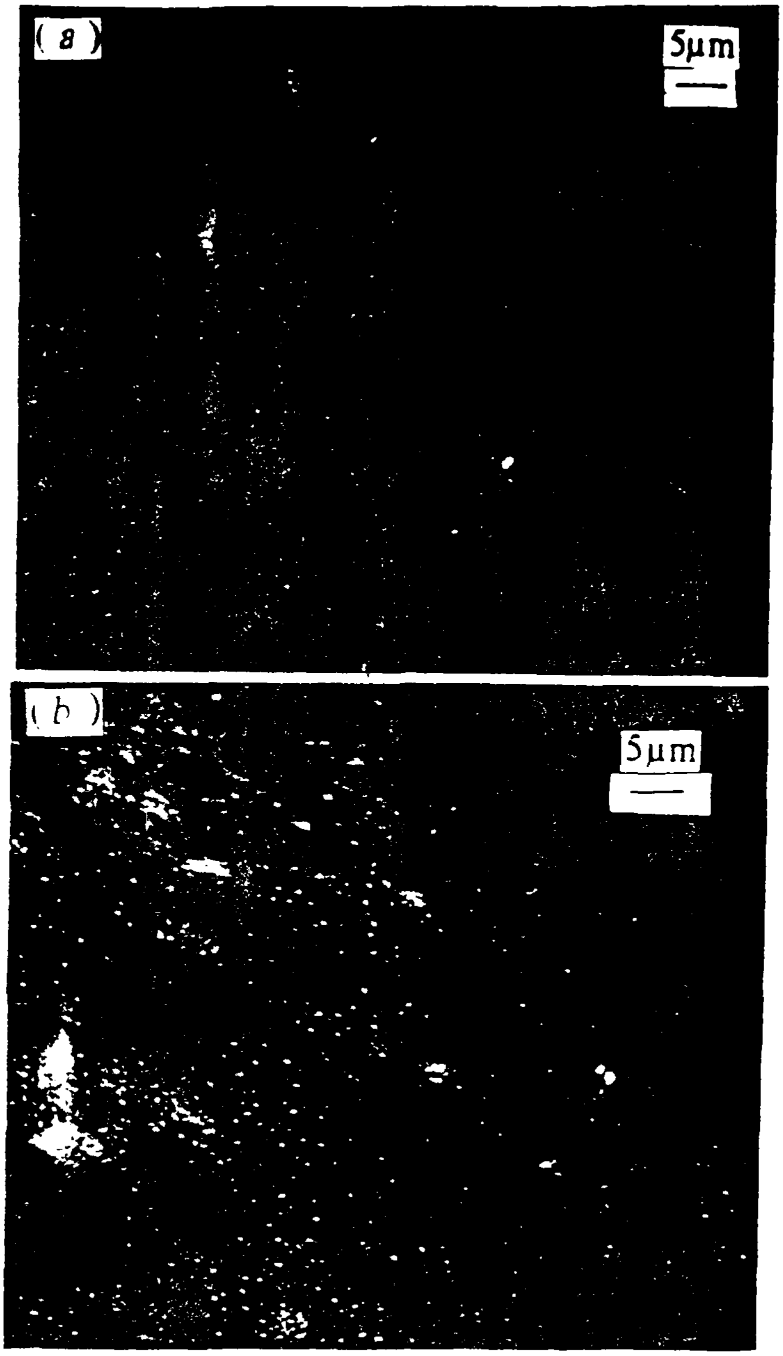

Fig 4

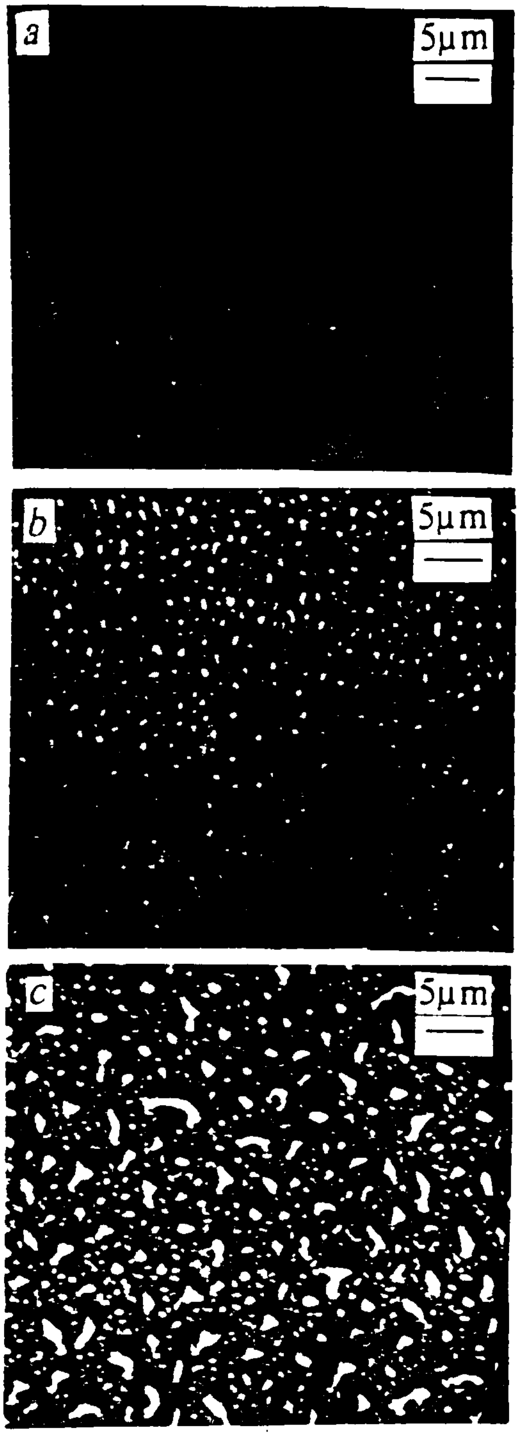

Fig 5

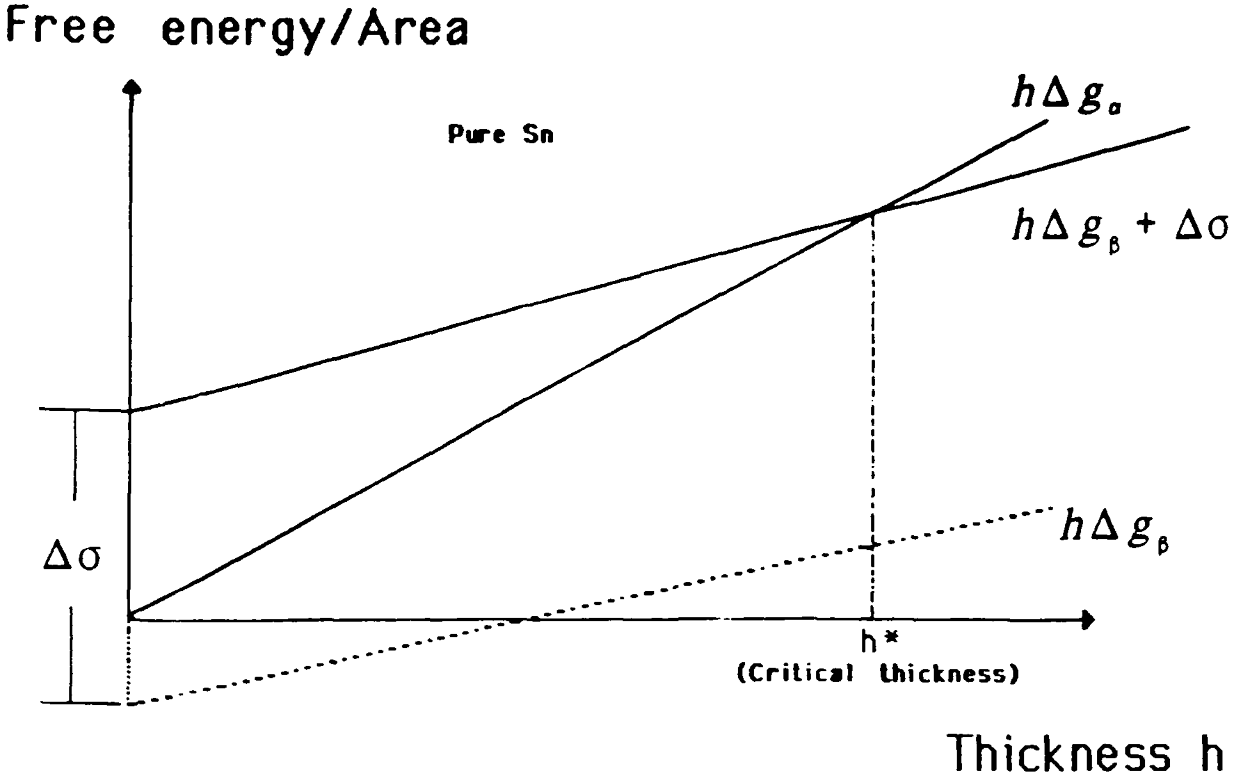
Free energy/Area
Pure Sn
$h\Delta g_\alpha$
$h\Delta g_\beta + \Delta\sigma$
$h\Delta g_\beta$
$\Delta\sigma$
h*
(Critical thickness)
Thickness h

Fig 6.

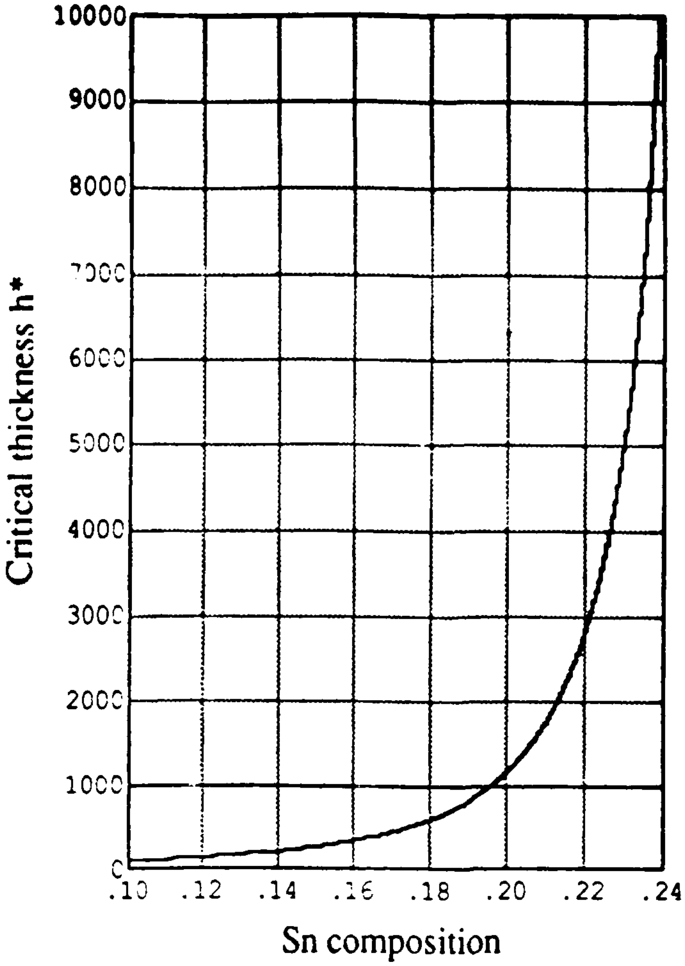
10000
9000
8000
7000
6000
5000
4000
3000
2000
1000
0
.10
.12
.14
.16
.18
.20
.22
.24
Critical thickness h*
Sn composition

Fig. 7

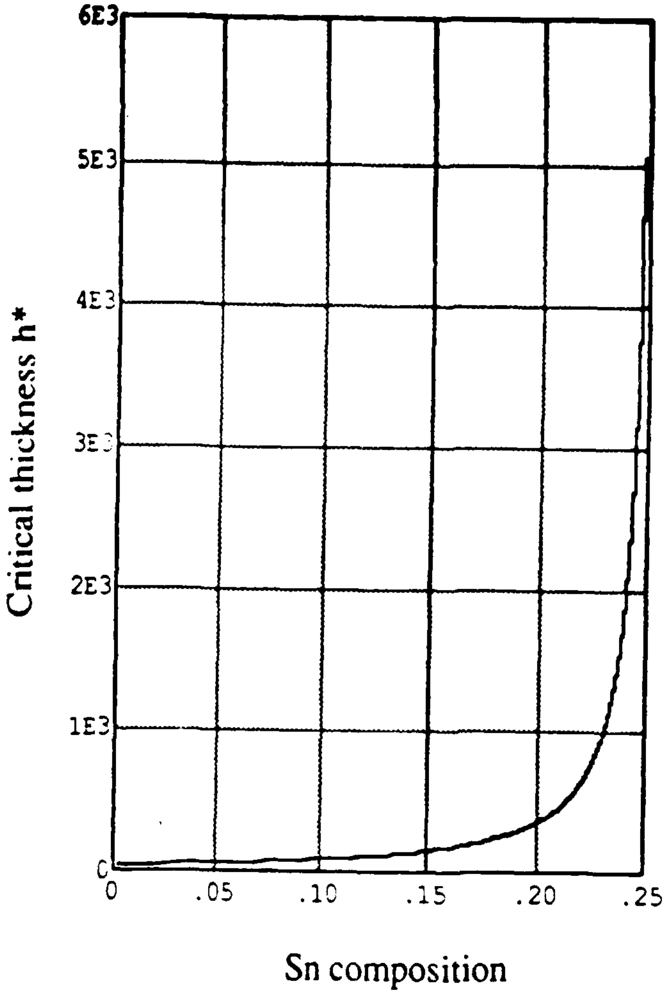
6E3
5E3
4E3
3E3
2E3
1E3
0
Critical thickness h*
0
.05
.10
.15
.20
.25
Sn composition

Fig. 8